Engineering Flat Bands in Twisted-Bilayer Graphene away from the Magic Angle with Chiral Optical Cavities

Cunyuan Jiang,[1,2,3] Matteo Baggioli,[1,2,3,*] and Qing-Dong Jiang[1,4,5,†]
[1]School of Physics and Astronomy, Shanghai Jiao Tong University, Shanghai 200240, China
[2]Wilczek Quantum Center, School of Physics and Astronomy, Shanghai Jiao Tong University, Shanghai 200240, China
[3]Shanghai Research Center for Quantum Sciences, Shanghai 201315,China
[4]Tsung-Dao Lee Institute, Shanghai Jiao Tong University, Shanghai 200240, China
[5]Shanghai Branch, Hefei National Laboratory, Shanghai 201315, China

(Received 13 June 2023; revised 17 September 2023; accepted 27 March 2024; published 18 April 2024)

Twisted bilayer graphene (TBG) is a recently discovered two-dimensional superlattice structure which exhibits strongly correlated quantum many-body physics, including strange metallic behavior and unconventional superconductivity. Most of TBG exotic properties are connected to the emergence of a pair of isolated and topological flat electronic bands at the so-called magic angle, $\theta \approx 1.05°$, which are nevertheless very fragile. In this work, we show that, by employing chiral optical cavities, the topological flat bands can be stabilized away from the magic angle in an interval of approximately $0.8° < \theta < 1.3°$. As highlighted by a simplified theoretical model, time reversal symmetry breaking (TRSB), induced by the chiral nature of the cavity, plays a fundamental role in flattening the isolated bands and gapping out the rest of the spectrum. Additionally, TRSB suppresses the Berry curvature and induces a topological phase transition, with a gap closing at the Γ point, towards a band structure with two isolated flat bands with Chern number equal to 0. The efficiency of the cavity is discussed as a function of the twisting angle, the light-matter coupling and the optical cavity characteristic frequency. Our results demonstrate the possibility of engineering flat bands in TBG using optical devices, extending the onset of strongly correlated topological electronic phases in moiré superlattices to a wider range in the twisting angle.

DOI: 10.1103/PhysRevLett.132.166901

Introduction.—Controlling and engineering quantum phases of matter is a central task in condensed matter physics. Inspired by the original discovery of single-layer graphene [1], two-dimensional (2D) materials have emerged as a versatile platform to realize strongly correlated physics in quantum many body systems [2]. Recently, unconventional superconductivity was discovered in twisted bilayer graphene (TBG), a two-dimensional superlattice where one layer of graphene is stacked on top of another at a special magic twisting angle, i.e., $\theta \approx 1.05°$ [3–6]. Galvanized by this breakthrough, several other stacked two-dimensional systems that host exotic superconductivity, such as twisted multilayer graphene, have been revealed [7–11]. While the underneath physical mechanism of superconductivity in twisted 2D systems is still under debate [12–19], it is clear that the isolated electronic flat bands appearing at the magical angle play an essential role. Besides superconductivity, flat bands are also indispensable for the emergence of strongly correlated insulating states and the strange-metal phase near the superconducting dome in the phase diagram of TBG, which closely mimics that of cuprate superconductors [20–28].

However, despite being a promising platform for studying strongly correlated physics, the unavoidable and uncontrollable nonuniformity of the twist angle across the sample, and the consequent difficulty in keeping the twist angle at its magic value, prevented a wide realization of these phenomena [29,30]. More precisely, since the magical-angle configuration is unstable, a little offset (around $\pm 0.1°$) of the twisting angle easily destroys most of the emergent exotic properties of TBG. In this regard, one of the most important challenges in the field is therefore to achieve superconductivity at nonmagic values of the twisting angle. To achieve this final goal, it is desirable to realize a primary step, namely, to create and stabilize electronic flat bands in a wider range of the twisting angle [31–35]. This will be the main purpose of our work.

In this Letter, we propose a new method to engineer stable flat bands at nonmagic angles by embedding twisted-bilayer graphene in a vacuum chiral cavity (see top panel in Fig. 1 for a cartoon of the setup). Using vacuum cavities to control materials and molecules has emerged as a fruitful playground connecting quantum optics to condensed matter and chemistry [36–42]. Floquet methods have also been proposed to engineer electronic properties in TBG [43,44] and have been experimentally applied in different contexts, e.g., Ref. [45]. However, because of the external electromagnetic radiation which drives the system out of equilibrium, this second route inevitably heats up the system, destroying

quantum coherence and inducing transient phenomena away from thermal equilibrium states. Therefore, it is unclear whether a stabilization of the flat bands in TBG using Floquet methods would preserve the related superconductivity properties. In this sense, at least in the case of TBG, optical methods might be superior. In the past, the usage of vacuum cavities has been proposed to design material conductivity [46,47], unconventional superconductivity [48–51], topological properties [52–55], and even chemical reactivity [56,57]. Some of these proposals have been already successfully realized experimentally.

A fundamental property of vacuum chiral cavities is that time-reversal symmetry is broken without the need of an external driving [36,37]. The same effect can be achieved using hBN encapsulation (e.g., [58]). Time-reversal symmetry breaking is essential since, as we will see, quantum fluctuations alone cannot significantly influence the electronic bands in TBG. In single-layer graphene, a band gap can be induced by quantum fluctuations in a chiral cavity as well [54]. However, the effect is too small to be directly observed due to the large bandwidth. As we will demonstrate, the situation is different in TBG near the magic angle, where the small bandwidth enables time-reversal symmetry-broken quantum fluctuations to play a significant role.

In recent years, a number of works have realized the vital impact of symmetry breaking on quantum-fluctuations-related phenomena, such as anomalous Casimir effects [59,60], topological gap generation [53,54], angular-momentum-dependent spectral shift [61], and selection of chiral molecules in chemical reactions [62–64]. A recent work by one of us [65] highlighted the combined power of symmetry breaking and quantum fluctuations, proving that symmetry breaking effects can be transmitted from a material to its vicinity by vacuum quantum fluctuations. In this scenario, the vacuum in proximity of a material with broken symmetries is referred to as its "quantum atmosphere".

In this Letter, we investigate the band renormalization of TBG due to the time-reversal symmetry broken quantum fluctuations in a chiral cavity. We start from a faithful tight-binding model of TBG and calculate the one-loop self-energy induced by the light-matter coupling. The bottom panel of Fig. 1 displays the specific Feynman diagram considered. We find that, for experimentally realizable values of the light-matter coupling and cavity frequency, the topological flat bands in TBG can be stabilized away from the magic angle in an interval of approximately $0.8° < \theta < 1.3°$. Our derivation and calculations can be directly generalized to other twisted 2D systems.

Setup and methods.—To set the stage, we model the Hamiltonian of the combined system, TBG, and cavity, as follows:

$$\hat{H} = \hat{H}_{\mathrm{TBG}}(\mathbf{q} - e\hat{\mathbf{A}}) + \hbar\omega_c \hat{a}^\dagger \hat{a}, \tag{1}$$

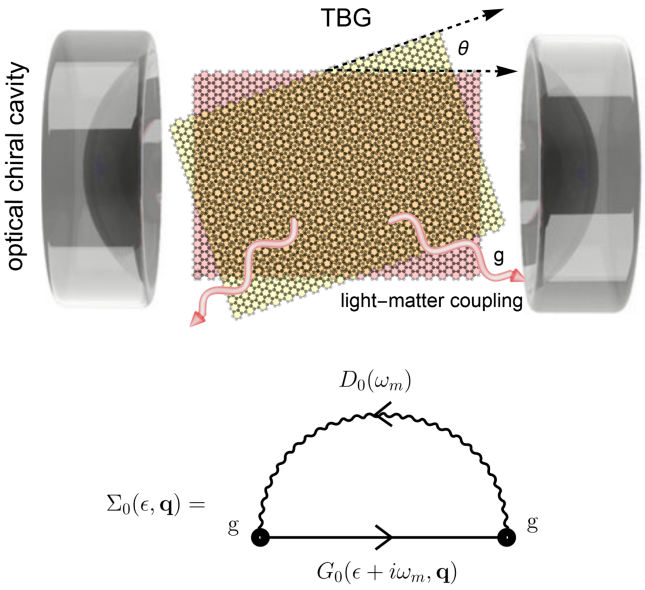

FIG. 1. Top panel. A cartoon of the optical setup considered in this work. Two skewed sheets of graphene are stacked on top of each other with a twisting angle θ creating a characteristic moiré pattern. They are then put inside a chiral optical cavity with a light-matter coupling g and a characteristic frequency ω_c. Bottom panel. The dominant Feynman diagram describing light-matter interactions in the optical chiral cavity and giving rise to the self-energy $\Sigma_0(\epsilon, \mathbf{q})$.

where $H_{\mathrm{TBG}}(\mathbf{q})$ represents the TBG Hamiltonian in reciprocal space, and ω_c is the cavity photonic mode frequency. TBG and cavity photonic modes are coupled through Peierls substitution $\mathbf{q} \mapsto \mathbf{q} - e\hat{\mathbf{A}}$, where $\hat{\mathbf{A}}$ can be expressed in terms of photonic creation and annihilation operators, i.e., $\hat{\mathbf{A}} = A_0(\boldsymbol{\epsilon}^*\hat{a}^\dagger + \boldsymbol{\epsilon}\hat{a})$. Here, $\boldsymbol{\epsilon}$ is the polarization tensor of the cavity photonic modes and $A_0 = \sqrt{(\hbar/2\epsilon_0 V\omega_c)}$ is the mode amplitude in terms of the cavity volume V. We focus on chiral cavities where the photonic polarization is given by $\boldsymbol{\epsilon} = (1/\sqrt{2})(\mathbf{e}_x + i\mathbf{e}_y)$, with $\mathbf{e}_{x(y)}$ the unit vector in the $x(y)$ direction. Our setup can be straightforwardly generalized to the multimode case.

To be concrete, let us consider the effective tight-binding Hamiltonian $H_{\mathrm{TBG}}(\mathbf{q})$ [66]

$$\begin{pmatrix} H_1(\mathbf{q}) & T_{\mathbf{q}_b} & T_{\mathbf{q}_{tr}} & T_{\mathbf{q}_{tl}} & \cdots \\ T^\dagger_{\mathbf{q}_b} & H_2(\mathbf{q}-\mathbf{q}_b) & 0 & 0 & \cdots \\ T^\dagger_{\mathbf{q}_{tr}} & 0 & H_2(\mathbf{q}-\mathbf{q}_{tr}) & 0 & \cdots \\ T^\dagger_{\mathbf{q}_{tl}} & 0 & 0 & H_2(\mathbf{q}-\mathbf{q}_{tl}) & \cdots \\ \vdots & \vdots & \vdots & \vdots & \ddots \end{pmatrix}, \tag{2}$$

where $\mathbf{q}$ is the wave vector, and $H_{1,2}(\mathbf{q})$ indicate the Hamiltonian of the top and bottom layer, respectively. Moreover, we have defined

$$\mathbf{q}_b = \frac{1}{3}(\mathbf{b}_1^m - \mathbf{b}_2^m), \qquad \mathbf{q}_{tr} = \frac{1}{3}(\mathbf{b}_1^m + 2\mathbf{b}_2^m),$$
$$\mathbf{q}_{tl} = \frac{1}{3}(-2\mathbf{b}_1^m - \mathbf{b}_2^m), \tag{3}$$

where $\mathbf{b}_1^m$ and $\mathbf{b}_2^m$ are moiré reciprocal vectors. The twisting angle θ is hidden in these vectors; see Fig. 6.11 in Ref. [66] for more details. The hopping matrix elements are given by

$$T_{\mathbf{q}_b} = t\begin{pmatrix} u & u' \\ u' & u \end{pmatrix}, \qquad T_{\mathbf{q}_{tr}} = t\begin{pmatrix} ue^{i\phi} & u' \\ u'e^{-i\phi} & ue^{i\phi} \end{pmatrix},$$
$$T_{\mathbf{q}_{tl}} = t\begin{pmatrix} ue^{-i\phi} & u' \\ u'e^{i\phi} & ue^{-i\phi} \end{pmatrix}, \tag{4}$$

where the various parameters have been fixed to $u = 0.817$, $u' = 1$, $\phi = 2\pi/3$, and $t = 0.11$ is the hopping parameter. This choice takes into account the different interlayer coupling strength of AA and AB stacked regions [24] due to the surface relaxation effects and the consequent atomic corrugation [67,68]. For more details about the TBG Hamiltonian we refer to the Supplemental Material [69]. Once the effective Hamiltonian is known, the bare electron propagator can be obtained using [54]

$$G_0^{-1}(\epsilon, \mathbf{q}) = [(\epsilon + i0^+)\mathbf{I} - H_{\mathrm{TBG}}(\mathbf{q})]^{-1}. \tag{5}$$

The full electron propagator, taking into account the interactions with the vacuum cavity, can then be derived from the Dyson equation

$$G^{-1}(\epsilon, \mathbf{q}) = G_0^{-1}(\epsilon, \mathbf{q}) - \Sigma_0(\epsilon, \mathbf{q}), \tag{6}$$

where Σ_0 is the self-energy (see bottom panel of Fig. 1) given by

$$\Sigma_0(\epsilon, \mathbf{q}) = -\frac{g^2}{\beta}\sum_{m=1}^{\infty} G_0(\epsilon + i\omega_m, \mathbf{q}) D_0(\omega_m). \tag{7}$$

Here, $\omega_m = 2\pi m k_B T$ is the mth Matsubara frequency and $g = v_F e A_0$ denotes the electron-photon coupling strength with v_F the Fermi velocity of monolayer graphene and e the electromagnetic coupling. For convenience, we define the dimensionless coupling $\tilde{g} \equiv g/k_B T$. Finally, $D_0(\omega_m)$ is the photon propagator given by

$$D_0(\omega_m) = \begin{pmatrix} \frac{-1}{i\omega_m + \omega_c} & 0 & \cdots \\ 0 & \frac{1}{i\omega_m - \omega_c} & \cdots \\ \vdots & \vdots & \ddots \end{pmatrix}, \tag{8}$$

with ω_c the cavity frequency. It should be noticed here that all quantities G_0, G, D_0, Σ_0 are matrices with the same dimension of the effective TBG Hamiltonian. With the full propagator in Eq. (6), the spectral function, giving the renormalized electronic band structure, can be calculated from

$$A(\epsilon, \mathbf{q}) = -\frac{1}{\pi}\mathrm{Im}\mathrm{Tr}G(\epsilon, \mathbf{q}). \tag{9}$$

More details about the TBG Hamiltonian, the structure in reciprocal space and the numerical methods employed can be found in the Supplemental Material [69].

Electronic spectrum.—It is well known that TBG exhibits a pair of topological flat bands at the magic angle, $\theta \approx 1.05°$ [70–72], which play a key role for the underlying strongly correlated physics. In panels (a) and (c) of Fig. 2, we show two examples of the electronic spectrum of TBG at, respectively, $\theta = 0.8°$ and $\theta = 1.5°$. As already mentioned, no isolated flat bands are present anymore in the electronic spectrum just moving of $\pm 0.3°$ from the magic angle. In other words, the flat bands are very fragile and sensitive to the twisting angle. In panels (b) and (d) of Fig. 2, we show the same electronic spectra in the presence of the chiral optical cavity, with a coupling $\tilde{g} = 2$ and a characteristic frequency $\omega_c = 0.3$ eV. The strength of this coupling corresponds to a micrometer-sized cavity, well within experimental reach, as demonstrated by a similar experimental value in [73]. A pair of nearly flat bands reappear away from the magic angle thanks to the coupling to the chiral cavity. Importantly, the two bands are not anymore degenerate as their energy is shifted from the Fermi energy and grows with the light-matter coupling $\tilde{g}$.

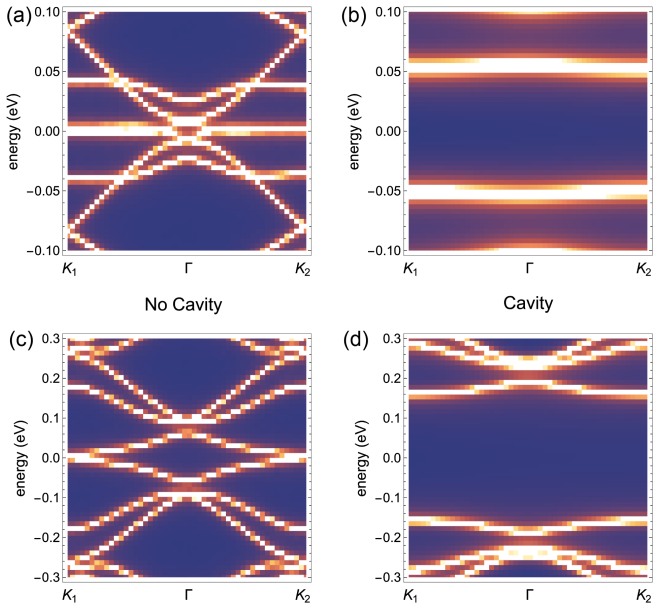

FIG. 2. The spectral function $A(\epsilon, q)$ showing the band structure of TBG with different light-matter coupling strength g and twisting angle θ. (a): $\theta = 0.8°$, $\tilde{g} = 0$; (b): $\theta = 0.8°$, $\tilde{g} = 2$; (c): $\theta = 1.5°$, $\tilde{g} = 0$; (d): $\theta = 1.5°$, $\tilde{g} = 2.5$. The optical cavity characteristic frequency is fixed to $\omega_c = 0.3$ eV.

This is a direct consequence of the breaking of time reversal symmetry induced by the chiral cavity. At the same time, the other bands, similarly to the case of the Dirac cone in monolayer graphene (see Supplemental Material [69]), are also gapped away as a result of the same symmetry breaking pattern.

Theoretical model and topological properties.—The emergence of the two isolated quasi-flat bands and their energy splitting, shown in Fig. 2, are intimately connected to the chiral nature of the optical cavity, which plays a fundamental role in this regard. To explicitly prove this statement, we construct a simplified analytical model which, as we will see, possesses all the minimal ingredients to describe our setup. In order to model the effects of the chiral cavity on TBG, we consider the following deformed Hamiltonian:

$$H_{\mathrm{TBG}+\tau}(\mathbf{q}) = H_{\mathrm{TBG}}(\mathbf{q}) + \tau \begin{pmatrix} \sigma_z & 0 & 0 & 0 & \cdots \\ 0 & \sigma_z & 0 & 0 & \cdots \\ 0 & 0 & \sigma_z & 0 & \cdots \\ 0 & 0 & 0 & \sigma_z & \cdots \\ \vdots & \vdots & \vdots & \vdots & \ddots \end{pmatrix}, \qquad (10)$$

where the coupling τ parametrizes the breaking of time-reversal symmetry on top of the original TBG Hamiltonian in Eq. (2). This is unlikely the most general deformation which breaks time-reversal symmetry, but it will be sufficient to qualitatively reproduce the numerical results displayed in Fig. 2 and identify the main underlying physical principle behind them. By diagonalizing the above Hamiltonian $H_{\mathrm{TBG}+\tau}(\mathbf{q})$, the band structure with broken time reversal symmetry can be obtained. The results are shown in Fig. 3 for different strength of the time-reversal symmetry breaking τ. As clearly demonstrated, the effects of τ is to gap away the higher energy bands and create a pair of isolated quasi-flat bands wth nondegenerate energy. At least at a qualitative level, these results are in perfect agreement with the more realistic scenario of TBG in a chiral cavity shown in Fig. 2, where the light-matter coupling $\tilde{g}$ plays an analogous role of the phenomenological parameter τ in Eq. (10). This simplified but tractable analytical model highlights the fundamental role of time reversal symmetry breaking, induced by the chiral cavity, in stabilizing the flat band of TBG. In order to characterize better the effects of the cavity, and of time-reversal breaking, on the electronic bands in TBG, we have computed the Berry curvature and the corresponding topological Chern number, that are geometrical properties of an energy band connected to how eigenstates evolve as a local function of parameters [74] (see Supplemental Material [69] for details).

At $\tau = 0$, all the bands are topologically trivial because of symmetry constraints. By introducing time-reversal

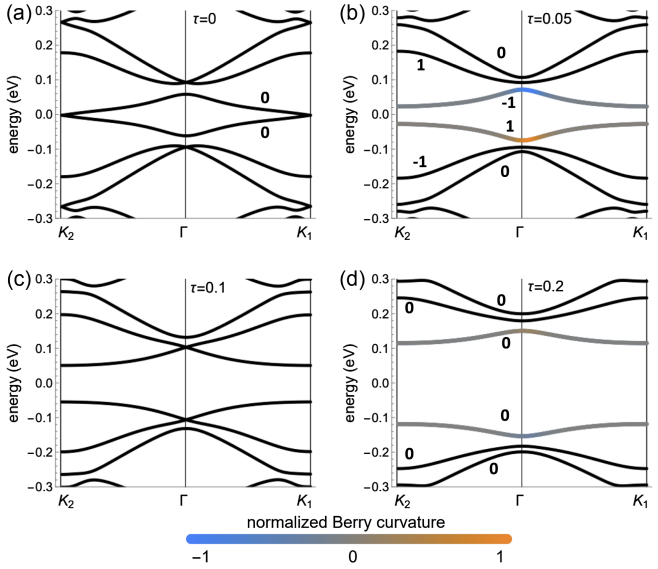

FIG. 3. The band structure of TBG at $\theta = 1.5°$ obtained from the deformed Hamiltonian in Eq. (10). Panels (a),(b),(c),(d), respectively, correspond to an increasing value for the time reversal breaking parameter $\tau = 0$, 0.05, 0.15, 0.2. The color scheme on top of the electronic bands in panels indicates the value of the reduced Berry curvature, and the integer numbers the Chern number of the lowest bands.

symmetry breaking, a gap at the K points opens between the two lowest bands and at the Γ point between the two consecutive ones. Qualitatively, for the two lowest bands, this mechanism is very similar to what is observed in single-layer graphene [44]. The bands becomes topological, with a finite ± 1 Chern number and a nontrivial Berry curvature exhibiting dipolar structure (Berry curvature dipole) [75]. By increasing τ further, the gap at the Γ point closes and the system undergoes a topological phase transition towards a topologically trivial state in which all electronic bands display a vanishing Chern number, as for $\tau = 0$. Despite the state is topologically trivial, the Berry curvature does not vanish identically in the whole Brillouin zone but displays an interesting dipolar structure. To the best of our knowledge, this topological phase transition in TBG induced by time reversal symmetry breaking was not discussed before. Importantly, the same behavior is also directly observed when TBG is coupled to the optical cavity (see Supplemental Material [69]), and it potentially represents a universal feature of TBG with broken time reversal symmetry that deserves further investigation.

Phase diagram and quasi-flat bands.—In order to explore the effects of the chiral cavity in more detail, we have performed an extensive analysis of the band structure for different values of θ and $\tilde{g}$ covering a wide range of the phase diagram around the magic-angle value. To give a quantitative estimate of the flatness of the bands, we define the energy bandwidth parameter

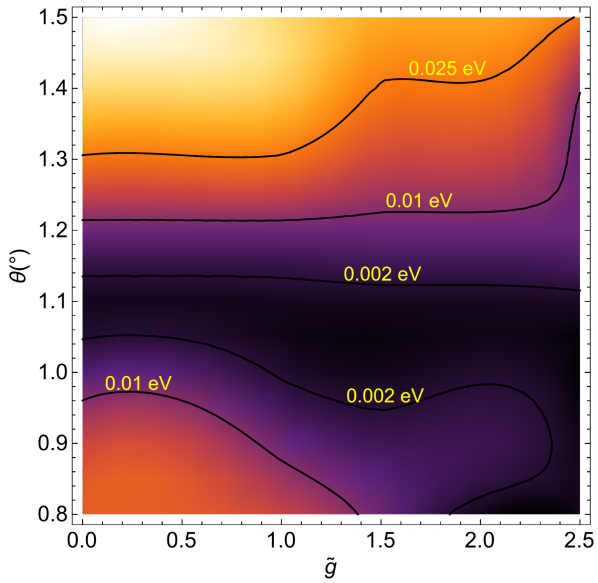

FIG. 4. The value of the energy bandwidth $\Delta\epsilon(\tilde{g},\theta)$ for different $\tilde{g}$ and θ. Darker color corresponds to a flatter band. The black solid lines indicate a few constant $\Delta\epsilon$ values as reference. The optical cavity frequency is set to $\omega_c = 0.3$ eV.

$$\Delta\epsilon(g,\theta) \equiv \epsilon_b^{\max}(g,\theta) - \epsilon_b^{\min}(g,\theta), \tag{11}$$

which quantifies the variation of the energy along the isolated nearly flat bands. As a reference, a completely flat band would correspond to $\Delta\epsilon(g,\theta) = 0$. Our results are shown in Fig. 4 in the interval $0.8° < \theta < 1.5°$ and $0 < \tilde{g} < 2.5$ for a fixed and reasonable value of the cavity characteristic frequency $\omega_c = 0.3$ eV. By increasing the value of the dimensionless coupling $\tilde{g}$, the energy bandwidth becomes smaller and therefore the isolated bands can be flattened away from the magic angle. As expected from simple intuition, the isolated bands can be flattened more efficiently for angles which are closer to the magic value. Interestingly, we find that it is easier to flatten the bands for angles smaller than the magic one compared to angles larger than the latter.

In general, we observe that "quasi-flat" bands, with a variation of the energy within 0.01 eV, can be easily tuned using reasonable values of the light-matter coupling $\tilde{g} \sim \mathcal{O}(1)$ for angles of $\pm 0.3°$ away from the magic value $\approx 1.05°$. Notice that, using the definition $g = \sqrt{(\hbar v_F^2 e^2 / 2\epsilon_0 V \omega_c)}$ and considering an optical cavity of volume $V = (1\ \mu\text{m})^3$, frequency of the order $\omega_c \approx 10^{-1}$ eV, and at a temperature of ≈ 1 K, this corresponds to a dimensionful light-matter coupling g of the order of $\approx 10^{-4}$ eV, which is certainly within experimental reach, as corroborated by existing literature [73,76,77]. Further elaboration on the experimental feasibility is provided in the Supplemental Material [69], which includes Refs. [78–80].

Conclusions.—In this Letter, we have revealed the possibility of extending the onset of topological flat bands in twisted bilayer graphene away from the magic angle by using optical chiral cavities. We have demonstrated that the effects of light-matter coupling can stabilize and flatten the topological flat bands for a large range of the twisting angle without the need of fine-tuning. Using physical values for the optical cavity frequency and the strength of the light-matter coupling, we have estimated that quasi-flat bands can be achieved at least in an interval of $0.8° < \theta < 1.3°$. From a theoretical point of view, taking advantage of a simplified analytical model, we have identified the breaking of time-reversal symmetry as the fundamental ingredient behind the achieved flattening, and the responsible of a previously overlooked topological phase transition.

One immediate future task is to verify whether all the interesting strongly-correlated physics related to the topological flat bands survive in presence of the chiral cavity or how that is modified. For example, it would be interesting to understand further the effects of time-reversal symmetry breaking on the emergent exotic superconductivity of TBG. Additionally, several works have emphasized the importance of quantum geometry in determining light-matter coupling strength in TBG. Therefore, a second task is to explore the role of quantum geometry in cavity-induced band renormalization in TBG [44,81,82]. The last and more pressing point is to verify our theoretical predictions within an experimental setup. Following our preliminary estimates (see more details in the Supplemental Material [69]), we conclude that the results shown in this Letter might already be within experimental reach.

In general, we expect the combination of twistronics and photonics engineering to become a powerful platform to study strongly correlated electronic systems and topological matter beyond the case of twisted bilayer graphene.

We would like to thank Dario Rosa for collaboration at an early stage of this project. We appreciate helpful discussions with Jinhua Gao and Miao Liang. We would like to thank the anonymous referees for several constructive comments. C. J. and M. B. acknowledge the support of the Shanghai Municipal Science and Technology Major Project (Grant No. 2019SHZDZX01). M. B. acknowledges the support of the sponsorship from the Yangyang Development Fund. Q.-D. Jiang was sponsored by National Natural Science Foundation of China (NSFC) under Grant No. 23Z031504628, Pujiang Talent Program 21PJ1405400, Jiaoda 2030 program WH510363001-1, and the Innovation Program for Quantum Science and Technology Grant No. 2021ZD0301900. Q.-D. Jiang was sponsored by the National Natural Science Foundation of China (NSFC) under Grant No. 12374332.

*b.matteo@sjtu.edu.cn
†qingdong.jiang@sjtu.edu.cn

[1] K. S. Novoselov, A. K. Geim, S. V. Morozov, D. Jiang, Y. Zhang, S. V. Dubonos, I. V. Grigorieva, and A. A. Firsov, Science **306**, 666 (2004).
[2] K. S. Novoselov, A. Mishchenko, A. Carvalho, and A. H. C. Neto, Science **353**, aac9439 (2016).
[3] Y. Cao, V. Fatemi, S. Fang, K. Watanabe, T. Taniguchi, E. Kaxiras, and P. Jarillo-Herrero, Nature (London) **556**, 43 (2018).
[4] M. Yankowitz, S. Chen, H. Polshyn, Y. Zhang, K. Watanabe, T. Taniguchi, D. Graf, A. Young, and C. Dean, Science **363**, eaav1910 (2019).
[5] X. Lu, P. Stepanov, W. Yang, M. Xie, M. A. Aamir, I. Das, C. Urgell, K. Watanabe, T. Taniguchi, G. Zhang, A. Bachtold, A. H. MacDonald, and D. K. Efetov, Nature (London) **574**, 653 (2019).
[6] Y. Saito, J. Ge, K. Watanabe, T. Taniguchi, and A. Young, Nat. Phys. **16**, 926 (2020).
[7] G. Chen, L. Jiang, S. Wu, B. Lyu, H. Li, B. L. Chittari, K. Watanabe, T. Taniguchi, Z. Shi, J. Jung, Y. Zhang, and F. Wang, Nat. Phys. **15**, 237 (2019).
[8] G. Chen, A. Sharpe, P. Gallagher, I. Rosen, E. Fox, L. Jiang, B. Lyu, H. Li, K. Watanabe, T. Taniguchi, J. Jung, Z. Shi, D. Goldhaber-Gordon, Y. Zhang, and F. Wang, Nature (London) **572**, 1 (2019).
[9] J. Park, Y. Cao, K. Watanabe, T. Taniguchi, and P. Jarillo-Herrero, Nature (London) **590**, 1 (2021).
[10] X. Zhang, K.-T. Tsai, Z. Zhu, W. Ren, Y. Luo, S. Carr, M. Luskin, E. Kaxiras, and K. Wang, Phys. Rev. Lett. **127**, 166802 (2021).
[11] J. Park, Y. Cao, L.-Q. Xia, S. Sun, K. Watanabe, T. Taniguchi, and P. Jarillo-Herrero, Nat. Mater. **21**, 877 (2022).
[12] H. C. Po, L. Zou, A. Vishwanath, and T. Senthil, Phys. Rev. X **8**, 031089 (2018).
[13] H. Isobe, N. F. Q. Yuan, and L. Fu, Phys. Rev. X **8**, 041041 (2018).
[14] F. Wu, A. H. MacDonald, and I. Martin, Phys. Rev. Lett. **121**, 257001 (2018).
[15] C. Xu and L. Balents, Phys. Rev. Lett. **121**, 087001 (2018).
[16] F. Xie, Z. Song, B. Lian, and B. A. Bernevig, Phys. Rev. Lett. **124**, 167002 (2020).
[17] Z.-D. Song and B. A. Bernevig, Phys. Rev. Lett. **129**, 047601 (2022).
[18] C.-C. Liu, L.-D. Zhang, W.-Q. Chen, and F. Yang, Phys. Rev. Lett. **121**, 217001 (2018).
[19] B. Roy and V. Juričić, Phys. Rev. B **99**, 121407 (2019).
[20] Y. Cao, V. Fatemi, A. Demir, S. Fang, S. L. Tomarken, J. Y. Luo, J. D. Sanchez-Yamagishi, K. Watanabe, T. Taniguchi, E. Kaxiras, R. C. Ashoori, and P. Jarillo-Herrero, Nature (London) **556**, 80 (2018).
[21] Y. Cao, D. Chowdhury, D. Rodan-Legrain, O. Rubies-Bigorda, K. Watanabe, T. Taniguchi, T. Senthil, and P. Jarillo-Herrero, Phys. Rev. Lett. **124**, 076801 (2020).
[22] X. Liu, Z. Wang, K. Watanabe, T. Taniguchi, O. Vafek, and J. Li, Science **371**, 1261 (2021).
[23] M. Xie and A. H. MacDonald, Phys. Rev. Lett. **124**, 097601 (2020).
[24] M. Koshino, N. F. Q. Yuan, T. Koretsune, M. Ochi, K. Kuroki, and L. Fu, Phys. Rev. X **8**, 031087 (2018).
[25] J. F. Dodaro, S. A. Kivelson, Y. Schattner, X. Q. Sun, and C. Wang, Phys. Rev. B **98**, 075154 (2018).
[26] N. F. Q. Yuan and L. Fu, Phys. Rev. B **98**, 045103 (2018).
[27] A. Thomson, S. Chatterjee, S. Sachdev, and M. S. Scheurer, Phys. Rev. B **98**, 075109 (2018).
[28] J. M. Pizarro, M. Calderón, and E. Bascones, J. Phys. Commun. **3**, 035024 (2019).
[29] J. M. Park, Y. Cao, L.-Q. Xia, S. Sun, K. Watanabe, T. Taniguchi, and P. Jarillo-Herrero, Nat. Mater. **21**, 877 (2022).
[30] J. H. Wilson, Y. Fu, S. Das Sarma, and J. H. Pixley, Phys. Rev. Res. **2**, 023325 (2020).
[31] Z. Bi, N. F. Q. Yuan, and L. Fu, Phys. Rev. B **100**, 035448 (2019).
[32] Y. W. Choi and H. J. Choi, Phys. Rev. B **100**, 201402(R) (2019).
[33] Y.-W. Liu, Y. Su, X.-F. Zhou, L.-J. Yin, C. Yan, S.-Y. Li, W. Yan, S. Han, Z.-Q. Fu, Y. Zhang *et al.*, Phys. Rev. Lett. **125**, 236102 (2020).
[34] A. O. Sboychakov, A. V. Rozhkov, A. L. Rakhmanov, and F. Nori, Phys. Rev. Lett. **120**, 266402 (2018).
[35] T. M. R. Wolf, J. L. Lado, G. Blatter, and O. Zilberberg, Phys. Rev. Lett. **123**, 096802 (2019).
[36] H. Hübener, U. De Giovannini, C. Schäfer, J. Andberger, M. Ruggenthaler, J. Faist, and A. Rubio, Nat. Mater. **20**, 438 (2021).
[37] F. Schlawin, D. M. Kennes, and M. A. Sentef, Appl. Phys. Rev. **9**, 011312 (2022).
[38] J. Bloch, A. Cavalleri, V. Galitski, M. Hafezi, and A. Rubio, Nature (London) **606**, 41 (2022).
[39] C. Valagiannopoulos, Phys. Rev. Appl. **18**, 044011 (2022).
[40] C. Schäfer, M. Ruggenthaler, and A. Rubio, Phys. Rev. A **98**, 043801 (2018).
[41] Z. Bacciconi, G. M. Andolina, T. Chanda, G. Chiriacò, M. Schiró, and M. Dalmonte, SciPost Phys. **15**, 113 (2023).
[42] A. Mercurio, G. M. Andolina, F. Pellegrino, O. Di Stefano, P. Jarillo-Herrero, C. Felser, F. H. Koppens, S. Savasta, and M. Polini, Phys. Rev. Res. **6**, 013303 (2024).
[43] M. Vogl, M. Rodriguez-Vega, and G. A. Fiete, Phys. Rev. B **101**, 241408(R) (2020).
[44] G. E. Topp, G. Jotzu, J. W. McIver, L. Xian, A. Rubio, and M. A. Sentef, Phys. Rev. Res. **1**, 023031 (2019).
[45] Y. H. Wang, H. Steinberg, P. Jarillo-Herrero, and N. Gedik, Science **342**, 453 (2013).
[46] V. Rokaj, M. Ruggenthaler, F. G. Eich, and A. Rubio, Phys. Rev. Res. **4**, 013012 (2022).
[47] G. Moddel, A. Weerakkody, D. Doroski, and D. Bartusiak, Phys. Rev. Res. **3**, L022007 (2021).
[48] M. A. Sentef, M. Ruggenthaler, and A. Rubio, Sci. Adv. **4**, eaau6969 (2018).
[49] F. Schlawin, A. Cavalleri, and D. Jaksch, Phys. Rev. Lett. **122**, 133602 (2019).
[50] J. B. Curtis, Z. M. Raines, A. A. Allocca, M. Hafezi, and V. M. Galitski, Phys. Rev. Lett. **122**, 167002 (2019).
[51] A. Thomas, E. Devaux, K. Nagarajan, T. Chervy, M. Seidel, D. Hagenmüller, S. Schütz, J. Schachenmayer, C. Genet, G. Pupillo *et al.*, arXiv:1911.01459.
[52] C. Ciuti, Phys. Rev. B **104**, 155307 (2021).

[53] T. Espinosa-Ortega, O. Kyriienko, O. V. Kibis, and I. A. Shelykh, Phys. Rev. A **89**, 062115 (2014).
[54] X. Wang, E. Ronca, and M. A. Sentef, Phys. Rev. B **99**, 235156 (2019).
[55] F. Appugliese, J. Enkner, G. L. Paravicini-Bagliani, M. Beck, C. Reichl, W. Wegscheider, G. Scalari, C. Ciuti, and J. Faist, Science **375**, 1030 (2022).
[56] J. Galego, C. Climent, F. J. Garcia-Vidal, and J. Feist, Phys. Rev. X **9**, 021057 (2019).
[57] J. Galego, F. J. Garcia-Vidal, and J. Feist, Phys. Rev. X **5**, 041022 (2015).
[58] M. Long, P. A. Pantaleón, Z. Zhan, F. Guinea, J. Á. Silva-Guillén, and S. Yuan, npj Comput. Mater. **8**, 73 (2022).
[59] D. T. Butcher, S. Y. Buhmann, and S. Scheel, New J. Phys. **14**, 113013 (2012).
[60] Q.-D. Jiang and F. Wilczek, Phys. Rev. B **99**, 165402 (2019).
[61] Q.-D. Jiang, arXiv:2307.14964.
[62] Y. Ke, Z. Song, and Q.-D. Jiang, Phys. Rev. Lett. **131**, 223601 (2023).
[63] R. R. Riso, L. Grazioli, E. Ronca, T. Giovannini, and H. Koch, Phys. Rev. X **13**, 031002 (2023).
[64] N. Vu, G. M. McLeod, K. Hanson, and A. E. DePrince III, J. Phys. Chem. A **126**, 9303 (2022).
[65] Q.-D. Jiang and F. Wilczek, Phys. Rev. B **99**, 201104(R) (2019).
[66] G. Catarina, B. Amorim, E. V. Castro, J. M. V. P. Lopes, J. M. V. P. Lopes, and N. Peres, Twisted bilayer graphene: Low-energy physics, electronic and optical properties, in *Handbook of Graphene Set* (John Wiley & Sons, Ltd., New York, 2019), Chap. 6, pp. 177–231.
[67] K. Uchida, S. Furuya, J.-I. Iwata, and A. Oshiyama, Phys. Rev. B **90**, 155451 (2014).
[68] P. Lucignano, D. Alfè, V. Cataudella, D. Ninno, and G. Cantele, Phys. Rev. B **99**, 195419 (2019).
[69] See Supplemental Material at http://link.aps.org/supplemental/10.1103/PhysRevLett.132.166901 for more details on the setup considered, additional computations and further analysis.
[70] R. Bistritzer and A. H. MacDonald, Proc. Natl. Acad. Sci. U.S.A. **108**, 12233 (2011).
[71] E. Suárez Morell, J. D. Correa, P. Vargas, M. Pacheco, and Z. Barticevic, Phys. Rev. B **82**, 121407(R) (2010).
[72] E. Y. Andrei and A. H. MacDonald, Nat. Mater. **19**, 1265 (2020).
[73] B.-S. Song, S. Noda, T. Asano, and Y. Akahane, Nat. Mater. **4**, 207 (2005).
[74] D. Xiao, M.-C. Chang, and Q. Niu, Rev. Mod. Phys. **82**, 1959 (2010).
[75] I. Sodemann and L. Fu, Phys. Rev. Lett. **115**, 216806 (2015).
[76] C. Maissen, G. Scalari, F. Valmorra, M. Beck, J. Faist, S. Cibella, R. Leoni, C. Reichl, C. Charpentier, and W. Wegscheider, Phys. Rev. B **90**, 205309 (2014).
[77] A. Frisk Kockum, A. Miranowicz, S. De Liberato, S. Savasta, and F. Nori, Nat. Rev. Phys. **1**, 19 (2019).
[78] G. Scalari, C. Maissen, D. Hagenmüller, S. De Liberato, C. Ciuti, C. Reichl, W. Wegscheider, D. Schuh, M. Beck, and J. Faist, J. Appl. Phys. **113**, 136510 (2013).
[79] L. Mauro, J. Fregoni, J. Feist, and R. Avriller, Phys. Rev. A **107**, L021501 (2023).
[80] G. Jarc, S. Y. Mathengattil, A. Montanaro, F. Giusti, E. M. Rigoni, R. Sergo, F. Fassioli, S. Winnerl, S. Dal Zilio, D. Mihailovic *et al.*, Nature (London) **622**, 487 (2023).
[81] G. E. Topp, C. J. Eckhardt, D. M. Kennes, M. A. Sentef, and P. Törmä, Phys. Rev. B **104**, 064306 (2021).
[82] W. T. Tai and M. Claassen, arXiv:2303.01597.